A BIOMECHANICAL MODEL FOR NUMERICAL SIMULATION OF THE EFFECTS OF GRADUATED COMPRESSION STOCKINGS ON HUMAN CALVES

by

Lihuan ZHAO[a*], Yanyan LI[a], Silu LIU[a], Kejiang WANG[b], Jing YU[b], and Changjing LI[a]

[a]School of Textile Science and Engineering, Tiangong University, Tianjin, China
[b]Radiology Department, Tianjin Xiqing Hospital, Tianjin, China

Original scientific paper
https://doi.org/10.2298/TSCI2503719Z

Graduated compression stockings (GCS) have been employed for several decades to prevent and treat venous diseases of the lower extremities in humans. In order to investigate the mechanism of action of GCS on the lower extremity, a biomechanical model was constructed to simulate the magnitude and distribution of stresses exerted by GCS on the soft tissues, bones, and saphenous veins of the calf. The saphenous vein at the ankle was intercepted, and a flow-solid bidirectional coupling model was established to study the effects of GCS on blood flow return. The results demonstrate that the custom-made GCS can apply pressure to the calf in a manner that is consistent with the desired gradient distribution. The simulated and experimental values of the GCS exerting pressure on the calf surface exhibit a similar variation trend. Furthermore, the application of a GCS has been demonstrated to enhance blood return in the saphenous vein and to elevate the velocity of blood flow. The greater the external pressure applied to the calf, the greater the blood flow velocity of the vein in the calf. The discrepancy between the simulated and experimental values of the blood flow velocity is approximately 8%. The results provide valuable insights into the magnitude and distribution of pressure exerted by the GCS on each part of the calf, confirm the effectiveness of the GCS in promoting blood flow back to the calf veins, and lay the foundation for the accurate design and promotion of GCS.

Key words: *GCS, biomechanical model, numerical simulation, venous disorder, blood flow*

Introduction

Statistical data indicates that the prevalence of varicose veins ranges from 10% to 25%. Among individuals aged 18 to 54 years, the prevalence is approximately one-third [1]. Patients with severe varicose veins in the lower extremities exhibit a number of adverse effects, including skin atrophy, hyperpigmentation, eczema, and recurrent ulcers in the lower extremities. These effects have a significant impact on the health and quality of life of patients [2].

Patients with varicose veins that are not obvious in appearance but have uncomfortable symptoms can be treated with compression therapy by GCS [3]. Patients with obvious symptoms of varicose veins should be treated surgically, and postoperative use of GCS

* Corresponding authors e-mail: zhaolihuan@tiangong.edu.cn

as well as medication should be used to consolidate the efficacy of surgery [4]. The GCS apply maximum pressure on the ankle of the wearer, and the applied pressure gradually decreases from the ankle upward along the leg to conform to the environment of venous blood return, thus promoting venous blood return [5-8] and playing a role in preventing varicose veins in the lower extremities or reducing the incidence of post-operative varicose vein complications [5]. The magnitude and distribution of the garment pressure that GCS exert on the body are the main factors that affect the effectiveness of GCS for the prevention and treatment of varicose veins [6, 7]. Generally, GCS with progressive pressure gradients exert 100% of the pressure at the ankle, 80% at mid-calf and only 40% to 60% under the knee, which is partially determined according to China Textile Industry Standard *FZ/T 73031-2009 Compression stocking*.

The efficacy of GCS in the prevention and treatment of varicose veins and in promoting recovery from varicose vein surgery has been demonstrated in multiple studies [8-11]. Nevertheless, patients remain uncertain about the efficacy of GCS in preventing varicose veins. This may be due to the fact that the GCS currently available on the market are only available in a limited number of conventional sizes and are not tailored to perfectly fit the patient's lower extremities. Consequently, the applied garment pressure to the legs may not be accurate. Furthermore, patients are unable to discern the full impact of GCS on venous blood return. These circumstances may impede implementation and dissemination of GCS [12, 13].

To investigate the impact of GCS on human lower extremities, to provide theoretical support for the accurate design of GCS, and to promote the promotion and application of GCS, numerous scholars have dedicated significant efforts in this area. As a result of the limitations of garment pressure tester technology, which can only measure the pressures exerted by GCS on the surface of the human body and which is constrained to specific test locations, the results cannot fully reflect the magnitude and distribution of the garment pressure on the human body. In response to this challenge, many scholars have established biomechanical models and employed numerical simulation methods to study the effect of GCS on the surface and interior of the human lower extremities, and some research results have been obtained. Zhao *et al.* [14] employed computed tomography (CT) imaging data to construct a biomechanical model of the human arm, which was utilized to simulate the magnitude and distribution of pressure applied by a compression arm sleeve during wear. Dan and Shi [15] utilized CT scan data to construct a cross-sectional model of the female waist and a model of the waist of compression pants to simulate the pressure and comfort of the waistband of compression pants. Yu *et al.* [16] constructed a model of a human hand and a model of a pressure glove to study the inhibitory effect of pressure therapy on scar growth in burn patients. They simulated the magnitude and distribution of pressure exerted by the glove on the back of the hand to provide a reference for the design and development of pressure gloves. Rohan *et al.* [17] constructed a sliced model of the lower extremity to investigate the biomechanical effects of GCS and muscle contraction on the deep veins of the lower extremity. Ghorbani *et al.* [18] constructed a model of an adult male human lower extremity and a pressure garment, with the objective of simulating the interaction between the lower extremity and the pressure garment.

In the aforementioned studies, models of the human body have incorporated elements such as skin, muscle, bone, and other components. However, there have been no human biomechanical models that include blood vessels. At present, numerical simulations of GCS worn on the lower extremities are capable of simulating the dynamic stress and stress distribution on the skin surface, as well as stress and strain on the soft tissues and bones in the cross-section of a leg wearing a GCS. However, there is a paucity of research on the transfer of

stress from pressure on the surface of the body to the venous blood vessel wall and blood flow after stress is applied to the vessel wall. This information is essential for elucidating the effects of GCS on venous blood flow in the lower extremities, improving the accuracy of GCS design, and promoting the application of GCS.

Methods

In light of the aforementioned analysis, the calf area from the ankle to the knee has been identified as the primary focus of this study. This region is particularly susceptible to the development of varicose veins, which are most prevalent in the lower legs. Additionally, superficial varicose veins are commonly observed in the saphenous vein, making it an ideal target for extraction. The objective of this project is to construct a biomechanical model of the human lower extremities while wearing GCS. This model will then be used to simulate the magnitude and distribution of stress on soft tissues, bones, and saphenous vessels after wearing GCS on the lower legs. Moreover, the construction of a flow-solid coupling model of the saphenous vein allows for the investigation of the impact of wearing GCS on venous blood flow in the lower leg and the examination of the potential role of GCS in the treatment of varicose veins. Finally, the results are subjected to a validation process.

Finite element analysis of the interaction between lower leg and graduated compression stockings

Building a 3-D geometric model of the human calf

The experimental equipment was a Philips Multiva 1.5T, magnetic resonance imaging (MRI) system, which featured a 16-channel platform that enabled ultra-high resolution imaging, allowing for the visualization of vascular branches while simultaneously increasing the scanning speed. To perform the MRI program, the volunteer (female, healthy, normal leg form, no history of varicose vein disease, age 26 years old, height 168 cm, weight 55 kg) wore loose pants underneath and lay flat on the test bed with the heels of both feet elevated using a soft pad to ensure no contact between the legs and between the legs and the test bed to ensure the integrity of the leg shape. Following the scanning procedure, the raw data in DICOM format were obtained for the purpose of constructing the calf model. The MRI image data were imported into MIMICS 19.0 software, where they were subjected to image segmentation and model 3-D reconstruction, thereby yielding the 3-D solid models of bones, soft tissues, and blood vessels. Figure 1 illustrates the relationship between the position of the bones, blood vessels, and soft tissues of the lower leg and a schematic diagram of their positions following assembly.

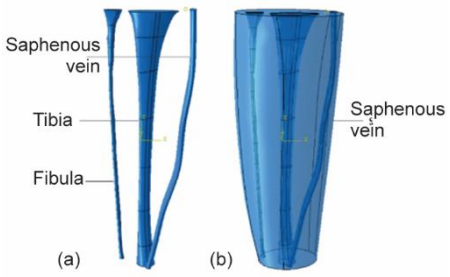

Figure 1. (a) Model of the tibia, fibula and saphenous vein and (b) schematic diagram of the position of the calf bones, blood vessels and soft tissues after assembly

Building 3-D geometric models of graduated compression stockings

Two types of GCS, classified as Class 1 and Class 2 in accordance with the FZ/T 73031-2009 standard, were selected as research samples due to their prevalence in clinical

applications. The volunteer was maintained in an upright position, and the circumferences of her leg were measured at four locations: the thinnest part of the ankle circumference was recorded as A, the transition between the Achilles tendon and the calf muscle was recorded as B, the largest part of the calf circumference was recorded as C, and the initial tibial ridge (below the knee) was recorded as D. The distance between adjacent measurement sites (recorded as L1, L2, and L3, respectively) was measured as shown in fig. 2. The measurement data were utilized to create Class 1 and Class 2 GCS using the compression garment design method previously studied by our research group [19]. Finally, the Class 1 and Class 2 GCS models were created in finite element software, respectively, and are presented in fig. 3.

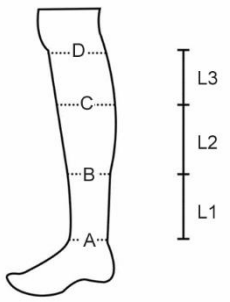

Figure 2. Schematic diagram of calf measurement position

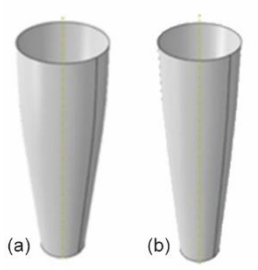

Figure 3. Custom-made compression stocking model; (a) custom-made Class 1 GCS and (b) custom-made Class 2 GCS

Defining material properties

In this study, bone was considered rigid and incompressible, and it was assumed to be free of deformation during wear. Soft tissue was defined as a homogeneous, isotropic, linear elastic material, while the GCS was defined as an isotropic, homogeneous elastomer. The material properties of the components are presented in tab. 1.

Table 1. Material properties of each component

Model name	Density [tone per mm^3]	Modulus of elasticity [MPa]	Poisson's ratio
Bone	$1.85 \cdot 10^{-9}$	7300	0.3
Vascular	$1.15 \cdot 10^{-9}$	50	0.45
Soft tissue	$1.00 \cdot 10^{-9}$	0.15	0.46
Compression stocking	$4.5 \cdot 10^{-10}$	0.49	0.32

Fluid-solid coupling simulation

In order to investigate the effect of GCS on blood flow [20] in the saphenous vein, the stress on the outer wall of the saphenous vein obtained from the finite element simulation in this study was applied to the outer side of the vessel wall in a flow-solid coupling model of the vessel. In this study, a 50 mm length of the vessel was intercepted at the ankle, which is the site where the GCS exerts the greatest pressure, in the saphenous vein of the lower leg. A flow-structure coupling model with a vessel wall thickness of 0.2 mm was then established. The stress values simulated in this study were applied to the exterior of the vessel wall in accordance with the aforementioned methodology.

The cross-sectional area and path of the reconstructed solid model of the saphenous vein were extracted based on the MRI data. The length of the vessel that was intercepted was 50 mm, and its cross-sectional shape was that of an ellipse. The short axis length was 3.5 mm, and the long axis length was 4.58 mm. The hollow vessel model with a wall thickness of 0.2 mm was obtained by sweeping the sketch tool, illustrated in fig. 4(a). The vessel was then filled with blood to create the blood model, which is shown in fig. 4(b).

Set-up of the solid field model

The vessel wall model was assigned material properties, including a density of 1050 kg/m³, a Young's modulus of 0.5 MPa, and a Poisson's ratio of 0.45. The vessel wall model was then meshed, with a mesh size of 0.4 mm being set. The entrance and exit of the vessel wall were fixed by inserting a displacement value, and the *X*-, *Y*-, and *Z*-components of the displacement were set to 0 by selecting the entrance and exit of the vessel wall. The fluid-solid coupling surface was established through the utilization of the *insert fluid solid interface* for the purpose of facilitating the transfer of loads between the blood and the vessel wall. Finally, a pressure was applied to set the pressure outside the vessel wall. This pressure was 2156 Pa, applied in the normal direction of the vessel wall to simulate the pressure of the vessel wall when wearing the custom-made primary GCS. When the custom-made Class 1 and Class 2 GCS were worn, the pressures were set to 2156 Pa and 3094 Pa, respectively, in order to simulate the pressures of the vessel wall.

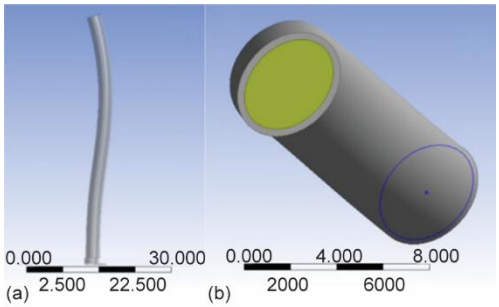

Figure 4. Saphenous vein model at the ankle; (a) vascular wall model and (b) blood model

Fluid field model set-up

The vessel inlet was designated as the *inlet*, and the vessel outlet was designated as the *outlet*. The mesh type was designated as tetrahedral mesh, and the mesh size was set to 0.2 mm.

The following steps were taken in the analysis of the fluid field settings: The type of model was designated as the viscous model *k*-*ε*. The blood density was set to 1050 kg/m^3, and the dynamic viscosity coefficient was 0.0035. The boundary conditions were established. A Philips Multiva1.5T MRI system was employed to ascertain the blood flow velocity of the saphenous vein in the volunteer's lower leg when in a supine position, resulting in a velocity of 0.033 m/s. The blood inflow velocity was set to 0.033 m/s. Given the low pressure within the vessel, the outlet pressure was set to 0 Pa, and the wall was set to static without slip. The surface of contact between the blood and the tube wall was selected using system coupling to create a dynamic grid region. Subsequently, the dynamic grid was established, the grid method of smoothness was selected, and the optimization method of spring/Laplace/boundary layer was employed for the purpose of achieving a smooth surface.

The validation of modelling by objective measurements

To validate the established biomechanical model, the tested values of garment pressure were compared with the simulated values. Furthermore, the peak blood return velocity in

the saphenous vein obtained from the vascular flow-solid coupling model was also compared with the data obtained from the MRI test.

Results and discussion

Numerical simulation of the interaction between the lower leg and GCS

Numerical simulation visualization

Figures 5 and 6 show the stress distributions of soft tissues, bones and saphenous vessels in the lower leg wearing custom-made Class 1 and Class 2 GCS, respectively.

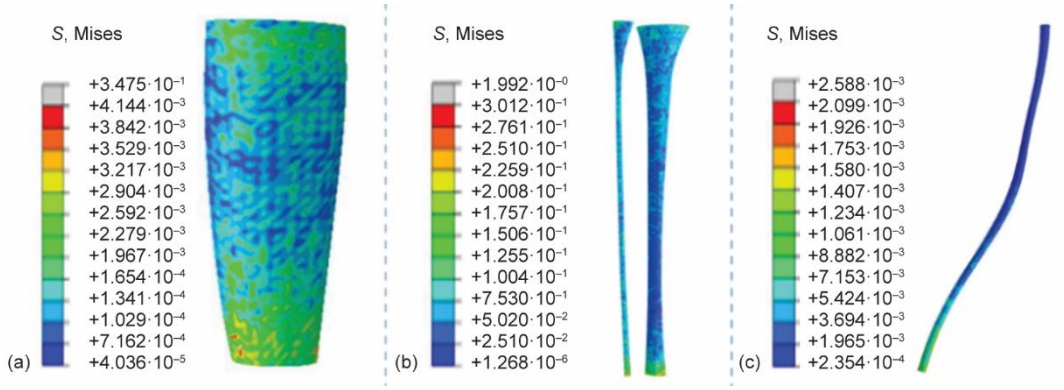

Figure 5. Stress cloud diagrams of soft tissue, bone, and saphenous vein after wearing custom-made Class 1 GCS; (a) stress of soft tissue, (b) stress of bones, and (c) stress of the saphenous vein

Figure 5(a) illustrates that following the application of a custom-made Class 1 GCS on the calf, a greater stress concentration was observed in the soft tissue at the ankle. The average stress value of the GCS acting on the soft tissue of the calf was within the range of 1.6-3 kPa. The average stress value of the GCS acting on the soft tissue at the ankle was 2.8 kPa, and gradually decreased along the calf. On the same cross-section, due to the influence of physiological structure, the stress values were greater close to the bones and in areas of greater curvature. As illustrated in fig. 5(b) the stress values on the tibia and fibula were in the range of 20-160 kPa after the calf model wore the custom-made Class 1 GCS. This indicated that the stress on the calf bones was significantly greater than that on the soft tissues when the GCS was worn. The fibula exhibited greater stress than the tibia, potentially due to the tibia surrounding soft tissue, which exerted greater pressure on the fibula when the soft tissue was compressed by the Class 1 GCS. The concentrated stress was observed in the ankles of the tibia and fibula, with some concentrated on the anterior side of the fibula due to the prominence of the tibia below the knee. In fig. 5(c), the stress applied to the soft tissue of the calf by the GCS was further transferred to the wall of the saphenous vein, which exhibited stress values in the range of 0.2-2 kPa. The stress was concentrated at the ankle of the saphenous vessel, showing a trend of gradually decreasing stress along the calf in an upward direction.

Figure 6(a) shows that after wearing a custom-made Class 2 GCS on the calf, the stress value of GCS acting on the soft tissue of the calf was in the range of 1-4 kPa, which was greater than the stress of wearing Class 1 GCS. The stress distribution on the soft tissues

of various parts of the calf was similar to wearing Class 1 GCS on the calf. As shown in fig. 6(b), the stress values on the tibia and fibula were in the range of 20-250 kPa after wearing the custom-made Class 2 GCS, and greater stress was concentrated at the ankle of the tibia and fibula. In fig. 6(c), the wall of the saphenous vein was subjected to stress values in the range of 0.5-3 kPa. Similarly, the greater stress was concentrated at the ankle of the saphenous vessel, and a trend of gradually decreasing stress along the calf upwards first could be observed.

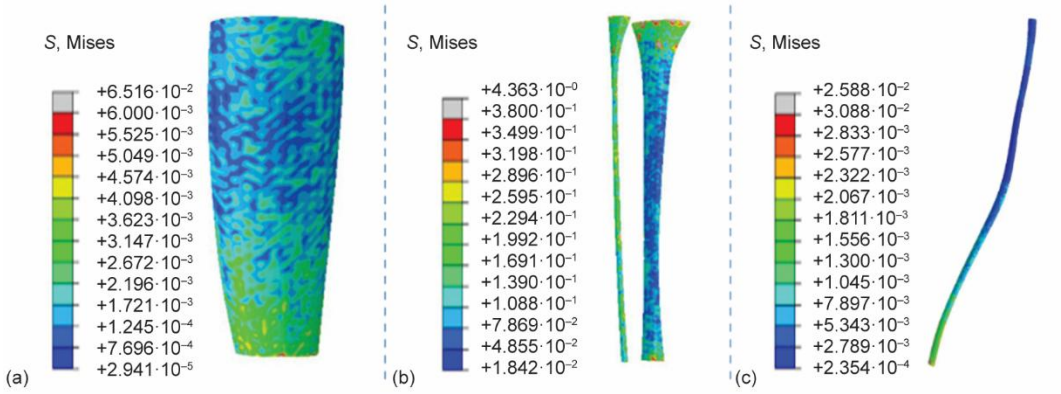

Figure 6. Stress cloud diagrams of soft tissue, bone, and saphenous vein after wearing custom-made Class 2 GCS; (a) stress of soft tissue, (b) stress of bones, and (c) stress of the saphenous vein

Validation of simulation results

The garment pressures of Class 1and Class 2 GCS were tested by Flexiforce A201 pressure sensor (TekScan, Boston, MA). Studies have shown that Flexiforce A201 sensor was used to evaluate the interface pressure, and had higher measurement accuracy [21]. The sensor was placed between the GCS and the calf of the volunteer, and garment pressure was tested at eight positions at even intervals on the four circumferences A, B, C, and D in fig. 2, and each position was tested three times.

According to the simulation results, the magnitude and distribution of the stresses on the soft tissues obtained from the finite element simulation after the calf model wore the GCS were similar to the results of the garment pressure test. To verify the simulation results, the average values of stresses on the four sections of A, B, C, and D on the calf soft tissue model were output, and the simulated values were compared with the actual garment pressures measured, fig. 7. The average distribution of stress in the four cross sections of the custom-made Class 1 and Class 2 GCS showed a gradient decrease, which was in accordance with the relevant product standards, and the error between the simulated and measured values was within 8%, and the measured and simulated values of the GCS were generally consistent.

To further investigate the magnitude and distribution of stresses transmitted by garment pressure to the saphenous vein vessels when GCS are worn on the surface of the human lower leg, eight sections were selected at equal intervals between the ankle and below the knee of the saphenous vein model, and the average stress values of each section were counted and output. The results are shown in fig. 8.

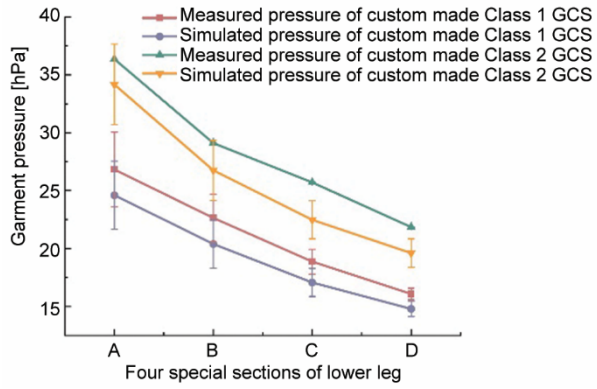

Figure 7. Comparison of the measured garment pressures and simulated stress values in the longitudinal direction of pressure stockings

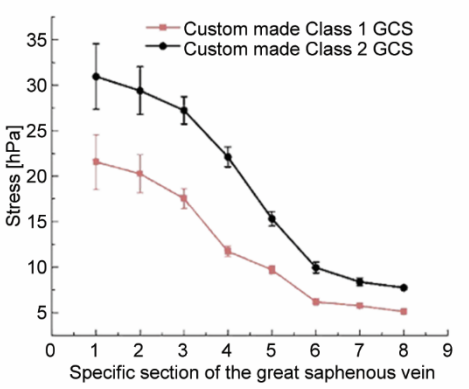

Figure 8. Mean value of the longitudinal section stress of the great saphenous vein simulated stress values in the longitudinal direction of pressure stockings

As shown in fig. 8, during the inwards transfer of pressure in the calf wearing the custom-made Class 1 GCS and the custom-made Class 2 GCS, the saphenous vein was subjected to maximum stress values of 21.56 hPa and 30.94 hPa at the ankle (1st) and minimum stress values of 5.12 hPa and 7.75 hPa at the knee (8th), respectively, along the longitudinal section of the calf. Custom-made Class 1 GCS and Class 2 GCS have the same trend of pressure distribution, with the Class 2 GCS having higher pressures than Class 1 GCS in all parts of the stocking. Overall, the garment pressure exerted by the GCS on the lower leg was transmitted to the saphenous vein, and the stress on the saphenous vein gradually decreased as the garment pressure decreased in steps from Section 1-8 of the saphenous vein.

Fluid-solid coupling simulation

The deformation of the saphenous blood vessel wall and its intravascular blood return in the lower leg after wearing the custom-made Class 1 and Class 2 GCS were simulated, and the results are shown in figs. 9 and 10, respectively.

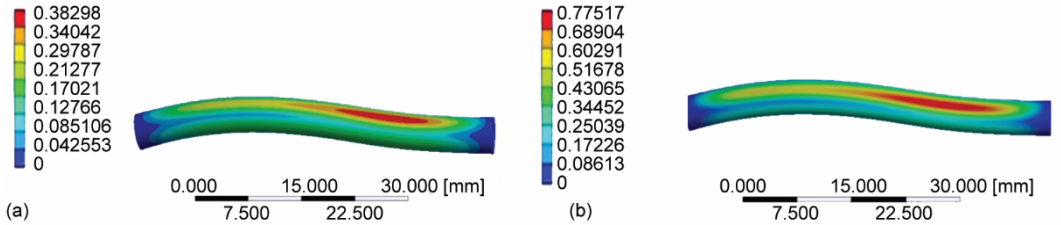

Figure 9. Wall deformation and distribution of great saphenous vein; (a) Class 1 GCS and (b) Class 2 GCS

When the human saphenous vein was modelled, the cross section of the vessel was not a regular circle. The shape of the cross section was nearly elliptical. When the human body is lying face upwards with the heel facing downwards and the toe upwards, the long axis of the elliptical cross-section of the vessel is parallel to the toe direction, and the short axis is perpendicular to the toe direction when viewed from the plantar direction. The strain of the

outer wall of the blood vessel at the ankle after wearing the Class 1 and Class 2 GCS had a similar change pattern. In this model, when the outer wall of the blood vessel was subjected to stress, a larger deformation was produced at the smaller diameter of the blood vessel or at the place where the curvature of the blood vessel was large. That is, a larger deformation was produced at the outer side of the entrance of the blood vessel as well as at the inner side of the exit due to the larger stress. In fig. 9, the displacement at the maximum deformation of the vessel wall was approximately 0.38 mm at the pressure value of 2156 Pa applied to the outer wall of the vessel, and the maximum displacement at the maximum deformation of the vessel wall was approximately 0.78 mm at the pressure value of 3094 Pa applied to the outer wall of the vessel.

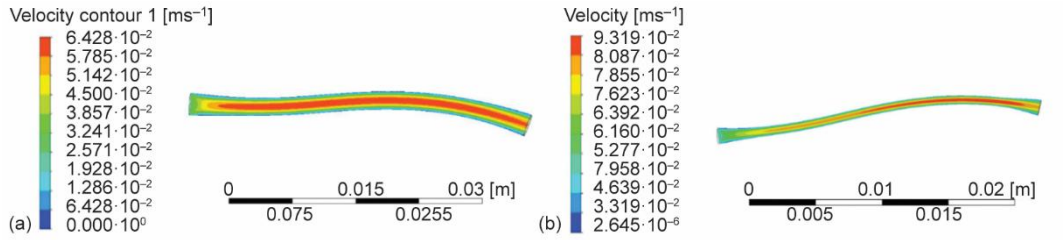

Figure 10. Great saphenous vein blood return; (a) Class 1 GCS and (b) Class 2 GCS

As shown in the cross section of the saphenous vein vessel in fig. 10, after the outer wall of the vessel was subjected to uniform pressure, due to the viscous nature of the fluid, layers of fluid underwent relative sliding when blood flowed in the vessel. That is, the phenomenon of laminar flow occurred, and during the flow process, the blood flowed at an inconsistent speed, and the blood flow was fastest in the central axis. When the human body wore the custom-made Class 1 GCS, the stress of the pressure transmitted to the saphenous vein wall at the ankle was 2156 Pa, the blood flow velocity at the entrance was 0.0338 m/s, and the peak blood flow velocity was 0.061 m/s. When the human body wore the custom-made Class 2 GCS, the stress of the saphenous vein vessel at the ankle was 3094 Pa, and the peak blood flow velocity was 0.091 m/s. This showed that the stress on the saphenous vein at the ankle increased as the GCS Class increased. The peak blood flow velocity of the saphenous vein at the ankle also increased, which confirmed that external pressure on the leg could increase the venous blood flow velocity and thus prevent and treat varicose vein disease.

Experimental verification

Experimental steps

First, the testers debugged the Philips Multiva 1.5T MRI System. Then, the volunteer wore the custom-made Class 1 GCS and rested flat on the test bed for 15 minutes. The volunteer assumed a proper posture with her legs slightly open, and her ankles rested soft cushions to keep them relaxed. The volunteer finished the preparation and started the scanning while wearing noise-proof ear muffs. The completion of the scanning was the completion of the first test. After the scan, the volunteer took off the custom-made Class 1 GCS, rested for 30 minutes and then wore the custom-made Class 2 GCS to prepare for the second test.

Before the test started, the volunteers put on the GCS and rested in a flat position on the test bed for 15 minutes to ensure the accuracy of the test.

Experimental results

The test results demonstrated that the peak blood return velocity in the saphenous vein was 0.065 m/s when the volunteer was wearing the custom-made Class 1 GCS and 0.099 m/s when the volunteer was wearing the custom-made Class 2 GCS. The simulated values were found to be smaller than the measured values, with a simulation error of approximately 8%. This indicates that the simulation results had some degree of reference value. These experimental results also demonstrated that the use of GCS can facilitate venous blood return and enhance the blood flow rate. It was observed that the greater the external pressure exerted on the calf, the greater the blood flow rate in the calf veins.

Conclusions

The results of the numerical simulations of the calf wearing GCS demonstrated that the garment pressure would be transmitted to the inner part of the calf, and that the bone would be subjected to significantly greater stress than the soft tissues and saphenous vessels due to the larger elastic modulus. The simulated stress values were then compared with the measured values of garment pressure. The trend of the simulated stress values and those of the measured garment pressure was essentially identical in the four cross-sections of the calf. The error was within 8%.

The results of the saphenous vein flow-solid coupling simulation model demonstrated that when the saphenous vein vessel wall was subjected to pressure, the vessel wall deformed, with the deformation being more pronounced at the larger curvature of the vessel wall. The deformation of the vessel wall may result in a reduction in the vessel caliber, which could subsequently lead to an acceleration of the venous return velocity. When the saphenous vein vessel was subjected to pressures of 2156 Pa and 3094 Pa, the simulated blood flow peaks were 0.061 m/s and 0.091 m/s, respectively, while the experimental peak saphenous vein blood flow velocities were 0.065 m/s and 0.099 m/s, respectively. A minor discrepancy was observed between the experimental and simulated values, which validated the reliability of the simulated outcomes. The results of the simulation and experimental studies demonstrated that the use of GCS can enhance venous blood return and elevate blood flow velocity. Furthermore, the results of this study demonstrated that an increase in external pressure applied to the calf resulted in a corresponding increase in blood flow velocity within the calf veins.

Acknowledgment

The authors would like to thank the financial support provided by the by China National Textile and Apparel Council, No. 2021065.

References

[1] Youn, Y. J., Lee, J., Chronic Venous Insufficiency and Varicose Veins of the Lower Extremities, *The Korean Journal of Internal Medicine*, *34* (2019), 2, pp. 269-283
[2] Ye, Z. D., *et al.*, Reflection and Evaluation of Minimally Invasive Treatment of Varicose Veins in the Lower Extremities, *Chin. J. Pract. Surg.*, *26* (2006), 10, pp. 2
[3] Guan, Y. B., Several Treatment Methods for Varicose Veins, *Chin. Arch. Gen. Surg.: Electron. Ed.*, *14* (2020), 1, pp. 4
[4] Sun, Y. C., *et al.*, Wearing State Based Pressure Distribution Study of Varicose Veins Care Compressive Stockings, *Knitting Industries*, (2018), 8, pp. 4

[5] Junior, O. A. S., *et al.*, Compression Stocking Prevents Increased Venous Retrograde Flow Time in the Lower Limbs of Pregnant Women, *Phlebology*, *35* (2020), 10, pp. 784-791
[6] Liu, X. F., *et al.*, Structural Characteristics and Research Progress of Medical Compression Stocking, *Prog. Biomed. Eng.*, *40* (2019), 2, pp. 78-82
[7] Yang, K., *et al.*, Development Status and Application of Graduated Compression Stockings, *Tech. Text.*, *37* (2019), 5, pp. 1-5,11
[8] Zolotukhin, I., *et al.*, A Randomized Trial of Class II Compression Sleeves for Full Legs *vs.* Stockings After Thermal Ablation with Phlebectomy, *J. Vasc. Surg.-Venous Lymphat. Dis.*, *9* (2021), 5, pp. 1235-1240
[9] Li, X. T., *et al.*, Varicose Veins of the Lower Extremity Secondary to Tricuspid Regurgitation, *Ann. Vasc. Surg.*, *60* (2019), Oct., pp. 477e1-477e6
[10] Chiang, N., *et al.*, Effects of Compression Therapy and Venous Surgery on Tissue Oxygenation in Chronic Venous Disease, *Phlebology*, *34* (2019), 7, pp. 474-480
[11] Bootun, R., *et al.*, Randomized Controlled Trial of Compression After Endovenous Thermal Ablation of Varicose Veins (COMETA Trial), *Ann. Surg.*, *273* (2021), 2, pp. 232-239
[12] Horner, J., *et al.*, Value of Graduated Compression Stockings in Deep Venous Insufficiency, *Br. Med. J.*, *280* (1980), 6271, pp. 820-821
[13] Zheng, Y. J., Tan, R., Research and Development of Health Care and Protective Function of Pressure Socks, *Wool. Text. J.*, *49* (2021), 11, pp. 75-80
[14] Zhao, L., *et al.*, A Three-Dimensional Biomechanical Model for Prediction of Garment Pressure in Pressure Therapy for Burn Patients, *Thermal Science*, *24* (2020), 4, pp. 2357-2365
[15] Dan, R., Shi, Z., Numerical Simulation of the Area Shrinkage Mass for the Waist of Elastic Pantyhose by Using FEM, *Int. J. Cloth. Sci. Technol.*, *32* (2020), 2, pp. 244-254
[16] Yu, A., *et al.*, Numerical Simulation of Pressure Therapy Glove by Using Finite Element Method, *Burns*, *42* (2016), 1, pp. 141-151
[17] Rohan, P.-Y., *et al.*, Prediction of the Biomechanical Effects of Compression Therapy on Deep Veins Using Finite Element Modelling, *Ann. Biomed. Eng.*, *43* (2015), 2, pp. 314-324
[18] Ghorbani, E., *et al.*, Finite Element Modelling the Mechanical Performance of Pressure Garments Produced from Elastic Weft Knitted Fabrics, *The Journal of The Textile Institute*, *110* (2018), 5, pp. 724-731
[19] Zhao, L. H., *et al.*, Compression Sleeves Design Based on Laplace Laws, *Journal of Textile Engineering & Fashion Technology*, *2* (2017), 2, pp. 314-320
[20] He, J.-H., *et al.*, Gold Nanoparticles' Morphology Affects Blood Flow near a Wavy Biological Tissue Wall: An Application for Cancer Therapy, *Journal of Applied and Computational Mechanics*, *10* (2024), 2, pp. 342-356
[21] Swanson, E. C., *et al.*, Evaluation of Force Sensing Resistors for the Measurement of Interface Pressures in Lower Limb Prosthetics, *J. Biomech. Eng.*, *141* (2019), 10, 101009

Paper submitted: October 4, 2023
Paper revised: March 15, 2024
Paper accepted: March 20, 2024
2025 Published by the Vinča Institute of Nuclear Sciences, Belgrade, Serbia.
This is an open access article distributed under the CC BY-NC-ND 4.0 terms and conditions.